

# Density-matrix renormalization study of the Hubbard model on a Bethe lattice

Marie-Bernadette Lepetit, Maixent Cousy and G. M. Pastor  
*Laboratoire de Physique Quantique, Unité Mixte de Recherche 5626 du CNRS,  
 118 route de Narbonne, F-31062 Toulouse, France*  
 (January 25, 2018)

The half-filled Hubbard model on the Bethe lattice with coordination number  $z = 3$  is studied using the density-matrix renormalization group (DMRG) method. Ground-state properties such as the energy  $E$ , average local magnetization  $\langle \hat{S}_z \rangle$ , its fluctuations  $\langle \hat{S}_z^2 \rangle - \langle \hat{S}_z \rangle^2$  and various spin correlation functions  $\langle \hat{S}_z(i) \hat{S}_z(j) \rangle - \langle S_z(i) \rangle \langle S_z(j) \rangle$  are determined as a function of the Coulomb interaction strength  $U/t$ . The calculated local magnetic moments  $\langle \hat{S}_z(i) \rangle$  increase monotonically with increasing Coulomb repulsion  $U/t$  forming an antiferromagnetic spin-density-wave state which matches the two sublattices of the bipartite Bethe lattice. At large  $U/t$ ,  $\langle \hat{S}_z(i) \rangle$  is strongly reduced with respect to the saturation value  $1/2$  due to exchange fluctuations between nearest neighbors (NN) spins ( $|\langle S_z(i) \rangle| \simeq 0.35$  for  $U/t \rightarrow +\infty$ ).  $\langle S_z(i)^2 \rangle - \langle S_z(i) \rangle^2$  shows a maximum for  $U/t = 2.4$ – $2.9$  which results from the interplay between the usual increase of  $\langle S_z(i)^2 \rangle$  with increasing  $U/t$  and the formation of important permanent moments  $\langle S_z(i) \rangle$  at large  $U/t$ . NN sites show antiferromagnetic spin correlations which increase with increasing Coulomb repulsion. In contrast next NN sites are very weakly correlated over the whole range of  $U/t$ . The accuracy of the DMRG results is discussed by comparison with tight-binding exact results, independent DMRG calculations for the Heisenberg model and simple first-order perturbation estimates.

## I. INTRODUCTION

Bethe lattices or Cayley trees have often been the basis of very attractive models for the theoretical study of various properties of solids. A Bethe lattice is completely characterized by the number of nearest neighbors  $z$  and by the lack of closed loops. The later feature simplifies calculations considerably allowing in many cases to obtain useful insights on the physics of complex problems, for example, in theory of many electron systems or in the theory of alloys and other disordered systems. Recently, the interest in the study of strongly correlated fermions on Bethe lattices has been renewed by the advances achieved in the limit of infinite spatial dimensionality ( $d \rightarrow \infty$ )<sup>1</sup>. Indeed, this lattice provides a systematic mean of realizing the  $d = \infty$  limit by letting  $z \rightarrow \infty$  and scaling the nearest neighbor (NN) hopping integrals as  $t = W/(4\sqrt{z})$ , where  $W$  refers to the band width. In this context, an important research effort has been dedicated to the half-filled Hubbard model. This concerns mainly the metal-insulator transition within the paramagnetic phase and also the properties of the antiferromagnetic phase which in the absence of frustrations is the most stable solution at low temperatures (bipartite lattice)<sup>2–4</sup>. Therefore, it would be of considerable interest to determine the properties of the half-filled Hubbard model on a Bethe lattice with finite  $z$  by using accurate numerical methods. Such

numerical studies could be very useful, particularly in view of the possibility of improving the  $z = \infty$  equations by introducing  $1/z$  corrections.

The aim of this paper is to determine several ground-state properties of the half-filled Hubbard model on a  $z = 3$  Bethe lattice as a function of the Coulomb interaction strength  $U/t$ . For this purpose we take advantage of a property that Bethe lattices share with one-dimensional (1D) chains, namely, the fact that there is only one path between any pair of sites in the system. This characteristic allows the design of a simple real-space renormalization scheme in order to apply the density-matrix renormalization group (DMRG) method<sup>5</sup>. Density-matrix renormalization is a very powerful technique which was first proposed a few years ago in the context of 1D spin systems. Since then it has been rapidly extended to become one of the leading numerical tools for the study of low-dimensional correlated quantum systems including recently two-dimensional lattices of finite size<sup>6</sup>. The success and wide range of applications found by this approach rely on two main qualities: its high accuracy even for systems as large as a few hundreds of sites, which allows safe extrapolations to the thermodynamic limit, and its flexibility concerning the model Hamiltonian under study (Heisenberg,  $t - J$ , Hubbard, Kondo, etc). However, except for the work of Otsuka on the spin-1/2  $XXZ$  Hamiltonian<sup>7</sup>, the infinite DMRG calculations have always been limited to 1D problems. To our knowledge, this is the first time that the DMRG algorithm for infinite systems is applied to a fermion model not having the 1D topology.

The remainder of the paper is organized as follows. In the next section the main details of the application of the DMRG method to the Bethe lattice are given. Results for the ground-state energy and several spin and charge local properties are presented and discussed in Sec. III. Finally, Sec. IV summarizes our conclusions.

## II. DETAILS OF THE CALCULATION

We consider the Hubbard Hamiltonian<sup>8</sup>

$$H = -t \sum_{\langle i,j \rangle, \sigma} \hat{c}_{i\sigma}^\dagger \hat{c}_{j\sigma} + U \sum_i \hat{n}_{i\uparrow} \hat{n}_{i\downarrow} \quad (1)$$

on a Bethe lattice with coordination number  $z = 3$  (see Fig. 1). In the usual notation,  $\hat{c}_{i\sigma}^\dagger$  ( $\hat{c}_{i\sigma}$ ) creates (annihilates) an electron with spin  $\sigma$  at site  $i$ ,  $\hat{n}_{i\sigma} = \hat{c}_{i\sigma}^\dagger \hat{c}_{i\sigma}$  is the number operator,  $t$  refers to the nearest neighbor (NN) hopping integral, and  $U$  to the on-site Coulomb repulsion.

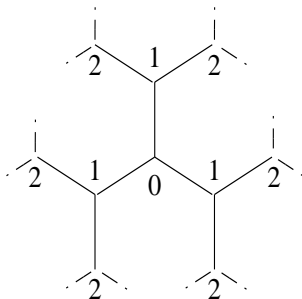


FIG. 1. Illustration of the Bethe lattice with coordination number  $z = 3$ . The numbers label non-equivalent sites.

Several ground-state properties of the Hubbard model are determined using the DMRG method<sup>5</sup>. This is an iterative projection technique which allows to include the most relevant part of the ground-state wave function on a limited number of many-body states. The system is partitioned into several regions in real space or blocks between which renormalized interactions are computed. The accuracy of the method is controlled by the number of states  $m$  retained for the description of each block. In the DMRG algorithm for infinite systems, the size of the system is increased at each renormalization step and the properties of the thermodynamic limit are determined by extrapolating the succession of finite system calculations.

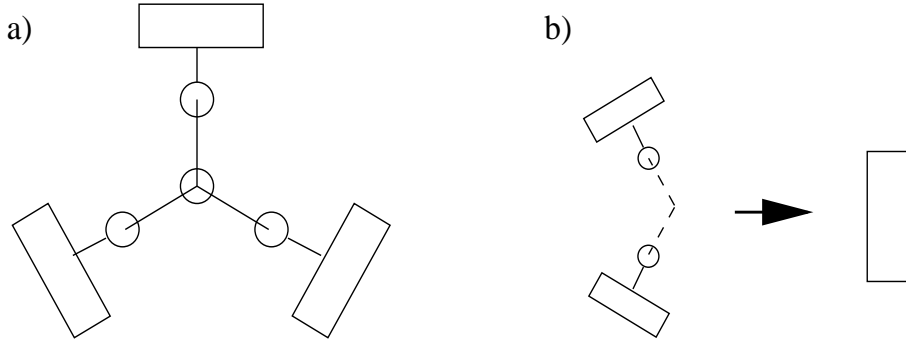


FIG. 2. (a) Renormalized Bethe lattice ( $z = 3$ , see Fig. 1) and (b) superblock renormalization procedure ( $\nu \geq 3$ ). Circles represent sites which are treated exactly and rectangles renormalized blocks. Notice that the total number of sites  $N_a = 3 \times 2^\nu - 2$  increases exponentially with the number of renormalization iterations  $\nu$ .

The renormalization procedure used for the  $z = 3$  Bethe lattice is illustrated in Fig. 2. Starting from a central site  $i = 0$  and the two shells of its first and second NN's, a new shell of NN's is added at each iteration  $\nu$ . The total number sites is thus given by  $N_a = 3 \times 2^\nu - 2$ . Notice the contrast with the usual DMRG scheme for 1D systems where  $N_a$  increases linearly with  $\nu$ <sup>5</sup>. The central site and its NN's (the sites on the first shell) are treated exactly at all iterations and the renormalizations are performed on the two branches which start at each of the first-shell sites (see Fig. 2). Notice that no renormalization is actually done until  $\nu = 3$ , i.e., the 10-site system with two sites in each block is treated exactly. In practice, the extrapolations of the considered properties to  $\nu \rightarrow \infty$  converge after  $\nu \simeq 15$  iterations. At this point  $N_a \simeq 2 \times 10^5$ . It should be however noted that in a Bethe lattice the surface to volume ratio does not vanish with increasing number of shells  $L$ . Taking into account that the number of sites in the  $l$ th shell is  $N_s = z(z-1)^{l-1}$  ( $l \geq 1$ ), one finds for  $z = 3$  that 1/2 of the sites belong to the outermost shell, 1/4 to the first shell below the surface, 1/8 to the second shell below the surface and so forth. Consequently, global properties of the system such as the average ground-state energy per site  $E_s$  are dominated by the outermost shells. Bulk properties corresponding to the translational invariant situation have to be calculated locally. For instance, the ground-state energy per site  $E$  is determined from  $E = U \langle \hat{n}_{0\uparrow} \hat{n}_{0\downarrow} \rangle + (zt/2) \sum_{\sigma} \langle \hat{c}_{1\sigma}^\dagger \hat{c}_{0\sigma} + \hat{c}_{0\sigma}^\dagger \hat{c}_{1\sigma} \rangle$  by using the density matrix reduced to the central sites  $i = 0$  and  $i = 1$  (see Fig. 1). In Sec. III it will be shown that the present DMRG algorithm yields accurate results for both global properties including the surface and local bulk-like properties.

For the calculations we take advantage of a theorem by Lieb which states that

for  $U > 0$  the ground-state spin  $S$  of the half-filled Hubbard Hamiltonian on a bipartite lattice is  $S = |N_A - N_B|/2$ , where  $N_A$  and  $N_B$  are the number of sites belonging to the two sublattices  $A$  and  $B$  ( $N_a = N_A + N_B$  even)<sup>9</sup>. In the Bethe lattice considered in this paper, even and odd shells constitute the two sublattices  $A$  and  $B$  (NN hopping). At the renormalization iteration  $\nu$  the ground-state spin is  $S = 2^{\nu-1}$  so that the calculations can be performed in the subspace of maximal  $S_z = S$ . This exact result provides an important simplification which appears to be crucial in order to achieve reliable results with present computer facilities, since for  $S_z = S$  the Hilbert space is much smaller than for  $S_z = 0$ . Thus, the number of states  $m$  kept in the renormalized blocks can be reduced significantly without loss of accuracy. For example for  $U = 0$ , we have performed DMRG calculations by using  $S_z = 0$  and  $S_z = S$ , keeping in both cases the same number of states  $m = 20$  in the renormalized blocks. After the first few iterations one finds important differences in the ground-state energy per site, the  $S_z = 0$  results being  $2.6 \times 10^{-2}t$  higher than those corresponding to  $S_z = S$ . Moreover, the sum  $P_m$  of the retained eigenvalues of the density matrix — a good criterion to estimate the quality of a DMRG calculation<sup>5</sup> — follows the same trend. Indeed, for  $S_z = S$ ,  $1 - P_m$  is always smaller than  $7 \times 10^{-4}$  while for  $S_z = 0$ ,  $1 - P_m$  can be as large as  $2 \times 10^{-2}$ , a value which in practice is too large for obtaining accurate results. In addition it should be noted that the uncorrelated limit is the most difficult case in DMRG calculations.  $1 - P_m$  is in fact always smaller for finite  $U/t$  than for  $U = 0$ <sup>11</sup>. The results presented in this paper were obtained by keeping  $m = 20$  states in each renormalized block. This would correspond to  $4^4 m^3 = 2,048,000$  possible configurations. However, only between 100,000–130,000 of them belong to the targeted  $S_z = S$  subspace. Still, the dimension of the superblock density-matrix,  $16m^2 = 6400$ , is quite important, which renders the computations very demanding.

### III. RESULTS AND DISCUSSION

In Fig. 3 results are given for the ground-state energy per site as a function of  $U/t$ .

Fig. 3 Lepetit et al.

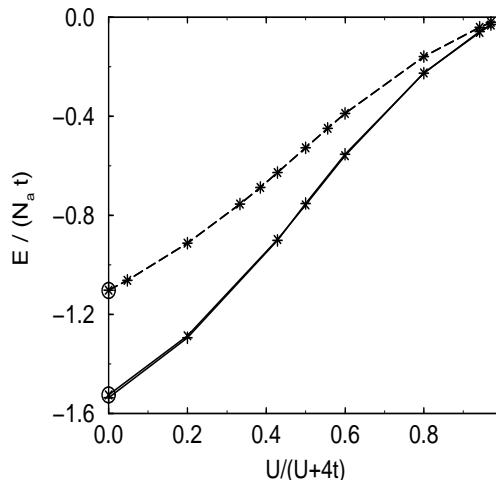


FIG. 3. Ground-state energy per site of the half-filled Hubbard model on a  $z = 3$  Bethe lattice as a function of the Coulomb repulsion  $U/t$ . The solid curve is calculated locally at the central sites from  $E = U\langle\hat{n}_{0\uparrow}\hat{n}_{0\downarrow}\rangle + (zt/2)\sum_{\sigma}\langle\hat{c}_{1\sigma}^{\dagger}\hat{c}_{0\sigma} + \hat{c}_{0\sigma}^{\dagger}\hat{c}_{1\sigma}\rangle$  (see Fig. 1). The dashed curve is the average energy  $E_s$  of the complete system including the surface. Crosses (plus signs) correspond to even (odd) renormalization iterations. The corresponding exact results for  $U = 0$  are given by the open circles.

Since in the Bethe lattice the weight of the atoms close to the surface does not vanish with increasing number of shells, it is necessary to discern between global properties which include surface contributions and local properties calculated close to the central site  $i = 0$ . The global energy  $E_s$  (dashed curve) is derived by extrapolating the ground-state energy per site for  $L \rightarrow \infty$ . For  $U = 0$  the DMRG calculations yield  $E_s = -1.10268t$ , while the exact results obtained by diagonalizing the finite- $L$  tight-binding matrix and extrapolating to  $L \rightarrow \infty$  is  $E_s^{ex} = -1.10306t$  (see Appendix). The agreement seems quite remarkable since  $E_s$  is given by the contributions of the atoms of the outermost shells —  $1/2$  of the sites belong to the surface,  $1/4$  to the layer below the surface, etc. — which are renormalized already from the very first iterations. Similarly good results are obtained for the local ground-state energy  $E$  (solid curve) which is obtained from the density matrices at the central sites extrapolated for  $L \rightarrow \infty$ . For  $U = 0$ , we obtain  $E = -1.5247t$ , while the integral of the single-particle density of states of the Bethe lattice is  $E^{ex} = -1.5255t$ . The renormalized blocks thus provide a proper embedding of the central sites. It is worth noting that the accuracy of these results, derived by keeping only  $m = 20$  states per block and setting  $S_z = S$  at each iteration, is comparable to the accuracy of calculations with  $m = 100$ – $150$  in the 1D Hubbard model ( $S_z = 0$ ). It goes without saying that  $m = 100$  calculations on a Bethe lattice are hardly feasible with present computer facilities. Since the uncorrelated limit is the most difficult (less precise) case in DMRG calculations on the Hubbard model<sup>11</sup>, we may expect that the results for finite  $U/t$  are at least as accurate. This is also confirmed by the sum  $P_m$  of the retained eigenvalues of the block density-matrix which increases with increasing  $U/t$ .

$E$  and  $E_s$  increase monotonously with  $U/t$  and vanish as expected in the Heisenberg limit. Their  $U/t$  dependence are very similar. In fact, allowing for a rescaling of the energies at  $U = 0$ ,  $E/E(U = 0)$  and  $E_s/E_s(U = 0)$  are close to the corresponding results for the 1D Hubbard chain<sup>10</sup>. Quantitatively,  $E_s$  is always higher than  $E$  due to surface boundary effects. Surface sites at the outermost shell have a smaller local coordination number  $z = 1$ . Therefore the effective local band width and the binding energy of surface sites are smaller than in the bulk.

Several local properties have been calculated around the central site  $i = 0$  in order to analyze the behavior of the ground-state in the bulk limit. Results for the average local magnetic moment  $\langle\hat{S}_z(0)\rangle$  are shown in Fig. 4.

Fig. 4 Lepetit et al.

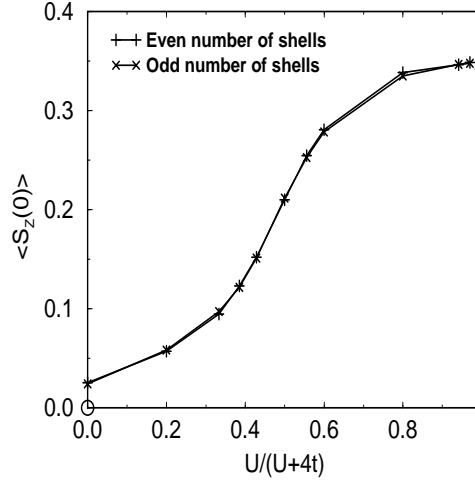


FIG. 4. Average magnetization  $\langle \hat{S}_z(0) \rangle$  for the half-filled Hubbard model on a Bethe lattice ( $z = 3$ ) calculated at the central site  $i = 0$ . Circles indicate tight-binding exact results ( $U = 0$ ) or perturbation theory estimates ( $U = \infty$ ). The dot is the DMRG result for the Heisenberg model on the  $z = 3$  Bethe lattice.

$\langle \hat{S}_z(0) \rangle$  increases monotonously with  $U/t$  reaching 0.35 in the Heisenberg limit. This reflects the formation of a spin-density wave (SDW) in which the average spins on the two sublattices  $A$  and  $B$  point in opposite directions. Indeed, for NN sites ( $i = 0$  and  $i = 1$ ) we obtain  $\langle \hat{S}_z(1) \rangle \simeq -\langle \hat{S}_z(0) \rangle$  and  $\langle \hat{S}_z(1') \rangle \simeq \langle \hat{S}_z(1) \rangle$  ( $|\langle \hat{S}_z(0) + \hat{S}_z(1) \rangle| \leq 10^{-4}$ ). Notice that the calculated  $\langle \hat{S}_z(0) \rangle$  does not vanish in the uncorrelated limit as it should. From the tight-binding solution for the Bethe lattice with a finite number of shells  $L$  one obtains  $\langle \hat{S}_z(0) \rangle = 1/(3L + 2)$  for  $L$  even and  $\langle \hat{S}_z(0) \rangle = 0$  for  $L$  odd (see the Appendix). Thus, in finite-size systems with even  $L$  the local magnetization does not vanish even for  $U = 0$  ( $S_z = S$ ). Our DMRG calculations follow precisely the exact results during the first renormalization iterations but for large  $\nu$  a slight increase of  $\langle \hat{S}_z(0) \rangle$  is observed for  $L$  odd which yields a small non-zero value in the extrapolation to  $L \rightarrow \infty$  ( $\langle \hat{S}_z(U=0) \rangle = 0.025$ ). We expect that this inaccuracy will be remedied by increasing the number of states kept in each renormalized block. In any case, since the DMRG method has better convergence properties with increasing  $U/t$ , the precision of the results improves rapidly for finite values of the interaction. In fact, in the strongly correlated limit the calculated  $\langle S_z(0) \rangle = 0.35$  is in very good agreement with perturbative estimations and with DMRG calculations using the Heisenberg Hamiltonian.

In order to analyze the strongly interacting Heisenberg limit we approximate the ground-state wave function by including first-order perturbations to the Néel state  $\phi_0$ :

$$\psi^{(1)} = \phi_0 - \frac{1}{2(z-1)} \sum_{\langle i,j \rangle} (S_j^+ S_i^- + S_j^- S_i^+) \phi_0. \quad (2)$$

Notice that the coefficient of the first-order correction (spin-flip states) is independent of the exchange constant  $J = 4t^2/U$ , since the off-diagonal matrix elements ( $J/2$ ) and the energy differences  $[2(z-1)J/2]$  are both proportional to  $J$  in the Heisenberg model. The average of local operators  $\hat{O}$  [e.g.,  $\hat{O} = \hat{S}_z(0)$  or  $\hat{O} = \hat{S}_z(0)\hat{S}_z(1)$ ] are obtained from

$$\langle \hat{O} \rangle = \frac{\text{Tr}[\hat{\rho} \hat{O}]}{\text{Tr}[\hat{\rho}]}, \quad (3)$$

where  $\hat{\rho}$  refers to the reduced density matrix. For example, for a single site Eq. (2) yields  $\rho(\uparrow, \uparrow) = 1$ ,  $\rho(\downarrow, \downarrow) = 3/16$  and  $\rho(\uparrow, \downarrow) = \rho(\downarrow, \uparrow) = 0$ . In this way one obtains  $\langle \hat{S}_z(i) \rangle = 13/38 = 0.342$ , which compares very well with the DMRG result  $\langle \hat{S}_z(i) \rangle = 0.348$  for  $U/t = 128$ . We conclude that the reduction of  $\langle \hat{S}_z(i) \rangle$  with respect to the saturation value  $1/2$  at very large  $U/t$  is the result of quantum spin fluctuations involving the first NN shell of atom  $i$ . In addition, we have also performed DMRG calculations for the Heisenberg model on the  $z = 3$  Bethe lattice which confirm the Hubbard results at  $U/t \gg 1$  [ $\langle \hat{S}_z(i) \rangle = 0.347$ , see Fig. 4].

Fig.5 Lepetit et al.

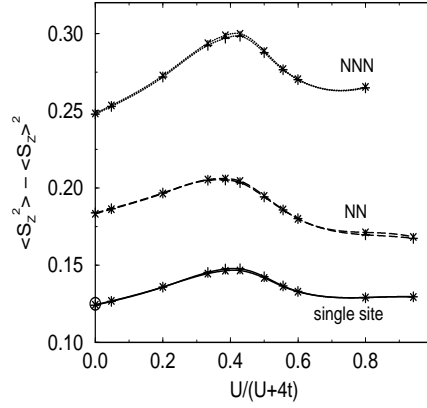


FIG. 5. Bethe-lattice results for the average spin fluctuations  $\langle \hat{S}_z^2 \rangle - \langle \hat{S}_z \rangle^2$  as a function  $U/t$ , where  $\hat{S}_z = \hat{S}_z(0)$  (single site, solid curve),  $\hat{S}_z = \hat{S}_z(0) + \hat{S}_z(1)$  (NN spins, dashed curve) and  $\hat{S}_z = \hat{S}_z(1) + \hat{S}_z(1')$  (NNN spins, dotted curve). See Fig. 1. Circles indicate tight-binding exact results ( $U = 0$ ) or perturbation theory estimates ( $U = \infty$ ). The dots are DMRG results for the Heisenberg model on the  $z = 3$  Bethe lattice.

Fig. 6 Lepetit et al.

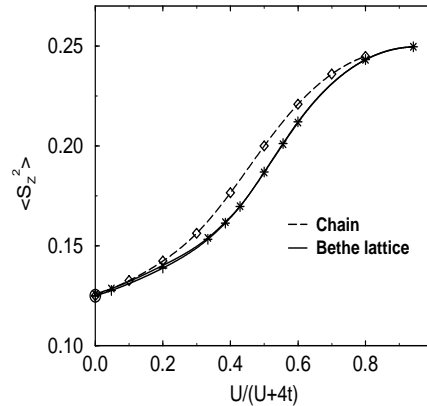


FIG. 6. Results for  $\langle \hat{S}_z(0)^2 \rangle$  of the half-filled Hubbard model as a function  $U/t$ . The solid curve corresponds to the  $z = 3$  Bethe lattice and the dashed curve to the one-dimensional chain ( $z = 2$ ).

In Fig. 5 results are given for the fluctuation of the local magnetic moments at a single site and at pairs of NN and NNN sites. In all cases  $\langle S_z^2 \rangle - \langle S_z \rangle^2$  presents a maximum for  $U/t = 2.4$ – $2.9$ . This behavior is a consequence of the interplay between the  $\langle S_z^2 \rangle$  increase which is due to the reduction of the weight of doubly occupied and empty sites by correlations, and the formation of permanent magnetic moments  $\langle S_z \rangle$ , which reduces the fluctuation of the spin moments around their average (see Fig. 4). As shown in Fig. 6,  $\langle S_z^2 \rangle$  in the Bethe lattice increases monotonously with  $U/t$  very much like in the 1D Hubbard chain. The main qualitative difference between Bethe-lattice and 1D results for  $\langle S_z^2 \rangle - \langle S_z \rangle^2$  comes from  $\langle S_z \rangle$  which is zero for the 1D case. Notice that the DMRG calculations are in good quantitative agreement with the tight-binding analytic results (open circles,  $U = 0$ ), with independent DMRG calculations for the spin-1/2 Heisenberg model (dots,  $U = \infty$ ) as well as with the first-order-perturbation estimation from Eqs. (2) and (3) (open circles,  $U = \infty$ ).

Fig. 7 Lepetit et al.

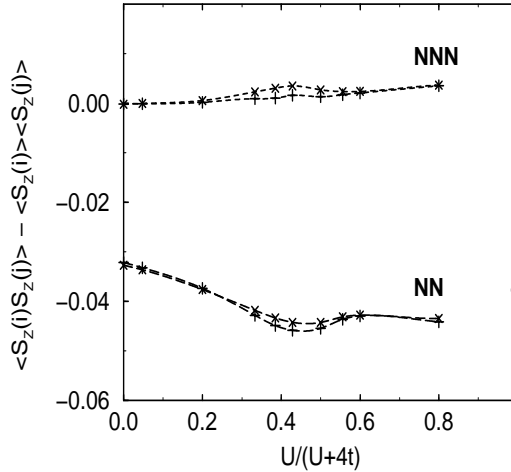


FIG. 7. Spin correlation functions  $\langle \hat{S}_z(i)\hat{S}_z(j) \rangle - \langle \hat{S}_z(i) \rangle \langle \hat{S}_z(j) \rangle$  between NN sites (dashed curve) and NNN sites (dotted curve). As in Fig. 5, circles indicate tight-binding exact results ( $U = 0$ ) or perturbation theory estimates ( $U = \infty$ ) and dots are DMRG results for the Heisenberg model.

The spin correlation functions  $\langle \hat{S}_z(i)\hat{S}_z(j) \rangle - \langle \hat{S}_z(i) \rangle \langle \hat{S}_z(j) \rangle$  between NN and NNN sites  $i$  and  $j$  are given in Fig. 7. NN spins show antiferromagnetic correlations which tend to become stronger as  $U/t$  increases. A shallow maximum is observed approximately at the same value of  $U/t$  for which  $\langle S_z^2 \rangle - \langle S_z \rangle^2$  is maximal. Notice that a considerable part of the antiferromagnetic correlations between NN is already present for  $U = 0$ . In contrast, the spin correlations between NNN's are much weaker. In this case, parallel alignment is slightly favored as  $U/t$  increases [ $\langle \hat{S}_z(1)\hat{S}_z(1') \rangle - \langle \hat{S}_z(1) \rangle \langle \hat{S}_z(1') \rangle > 0$ ]. These trends are consistent with the sign



alternations found in  $\langle \hat{S}_z(i) \rangle$  for  $i$  belonging to different sublattices (SDW). As expected, good agreement is obtained between the Hubbard results for large  $U/t$  and independent DMRG calculations for the Heisenberg model. The first-order estimates [Eq. (2)] are somewhat less accurate in this case but still remain qualitatively correct.

The average density  $\langle \hat{n}(i) \rangle$  at the central sites  $i = 0$  and  $i = 1$  is very close to 1 independently of  $U/t$ , which confirms the expected absence of a charge-density wave for  $U \geq 0$  ( $|\langle \hat{n}_{i\uparrow} + \hat{n}_{i\downarrow} \rangle - 1| < 10^{-4}$ ). The fluctuations of the density at a single site and at pairs of NN and NNN sites are given in Fig. 8.

Fig. 8 Lepetit et al.

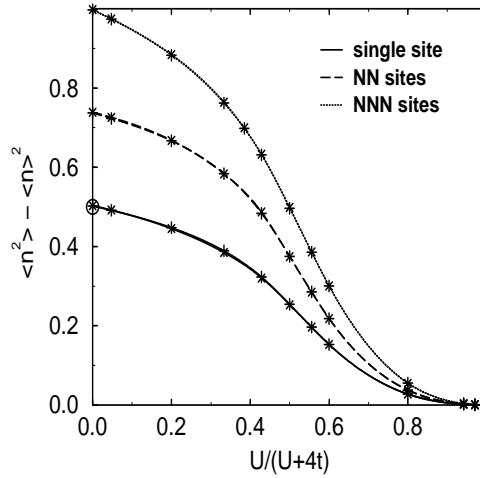


FIG. 8. Bethe-lattice results for the density fluctuations  $\langle \hat{n}^2 \rangle - \langle \hat{n} \rangle^2$  as a function  $U/t$ , where  $\hat{n} = \hat{n}(0)$  (single site, solid curve),  $\hat{n} = \hat{n}(0) + \hat{n}(1)$  (NN sites, dashed curve) and  $S_z = \hat{n}(1) + \hat{n}(1')$  (NNN sites, dotted curve).  $\hat{n}(i) = \hat{n}_{i\uparrow} + \hat{n}_{i\downarrow}$ , see Fig. 1.

In all cases we observe a monotonic crossover from the uncorrelated regime ( $\langle \hat{n}^2 \rangle - \langle \hat{n} \rangle^2$  maximal) to the strongly correlated, localized regime where charge fluctuations are suppressed. The  $U/t$  dependence is quite similar to what is obtained for 1D Hubbard model. The density fluctuation at a pair of NNN sites (dotted curve) is approximately twice the single-site result (solid curve) which indicates, as in the case of the spin degrees of freedom, that density correlations between NNN's are very weak [ $\langle \hat{n}(1)\hat{n}(1') \rangle - \langle \hat{n}(1) \rangle \langle \hat{n}(1') \rangle \simeq 0$ ]. In contrast, for NN sites charge fluctuations are significantly smaller. One observes that  $\langle [\hat{n}(0) + \hat{n}(1)]^2 \rangle - \langle \hat{n}(0) + \hat{n}(1) \rangle^2 \simeq (3/2)[\langle \hat{n}(0)^2 \rangle - \langle \hat{n}(0) \rangle^2]$  or equivalently  $\langle \hat{n}(0)\hat{n}(1) \rangle - \langle \hat{n}(0) \rangle \langle \hat{n}(1) \rangle \simeq [\langle \hat{n}(0)^2 \rangle - \langle \hat{n}(0) \rangle^2]/2$ . Notice that these relations hold approximately for all values of  $U/t$ , even for  $U = 0$ . The ratio between single-site charge fluctuations and fluctuations on a pair of NN's is not much affected by changes in the Coulomb repulsion strength and therefore seems to result mainly from the geometrical proximity of NN sites.

## IV. CONCLUSION

Several ground-state properties of the half-filled Hubbard model have been determined on the Bethe lattice with coordination  $z = 3$  by using a density-matrix renormalization group (DMRG) algorithm for open infinite systems. Though the lattice is not one dimensional (1D), the existence of a unique path between any pair of sites allows to formulate a simple renormalization procedure. In contrast to previous density-matrix renormalizations studies of Hubbard-like models on 1D chains or ladders where the number of sites  $N_a$  increases linearly with the number of iterations  $\nu$ , in the present approach  $N_a$  increases exponentially with  $\nu$  ( $N_a = 3 \times 2^\nu - 2$ ). This is a consequence of the fact that 2 blocks are renormalized into a single one at each iteration. Despite the very rapid increase of  $N_a$ , the DMRG method provides accurate results over the whole range of  $U/t$  already by keeping few states per block ( $m = 20$ ). This is achieved by working in the subspace of maximal spin projection  $S_z = S$ , where the ground-state spin  $S = 2^{\nu-1}$  is derived from a theorem by Lieb<sup>9</sup>. For example, in the limit of  $U = 0$  the calculated ground-state energy per site differs by only  $3 \times 10^{-4}t$  from the exact tight-binding result. It is remarkable that this level of precision concerns not only local properties calculated at the unrenormalized central sites, but also global properties which are dominated by the renormalized sites of the outermost shells. From a general point of view, the present study encourages renormalizations of more than one block into a superblock in future DMRG algorithms.

The main results for the  $z = 3$  Bethe lattice may be summarized as follows. The calculated local magnetic moments  $\langle \hat{S}_z(i) \rangle$  increase monotonically with increasing Coulomb repulsion  $U/t$  forming an antiferromagnetic spin-density-wave state which matches the two sublattices of the bipartite Bethe lattice. The maximum  $\langle \hat{S}_z(i) \rangle$  found in the Heisenberg limit ( $\langle \hat{S}_z(i) \rangle = 0.35$ ) is reduced with respect to the saturation value  $\langle \hat{S}_z(i) \rangle = 1/2$  as a result of exchange flips between the spin at site  $i$  and its NN's that point in opposite directions. The fluctuations of the local spins  $\langle S_z(i)^2 \rangle - \langle S_z(i) \rangle^2$  show a maximum as a function of  $U/t$  for  $U/t = 2.4$ – $2.9$ . For small  $U/t$  the usual increase of  $\langle S_z(i)^2 \rangle$  due to the reduction of double occupations dominates, while for large  $U/t$  the formation of large permanent moments  $\langle S_z(i) \rangle$  blocks local spin fluctuations. NN sites show important antiferromagnetic spin correlations which increase with increasing Coulomb repulsion. However, NNN sites are very weakly correlated over the whole range of  $U/t$ . The AF correlations are very short ranged in contrast to the static picture of a SDW. This reflects the importance of quantum fluctuations in the  $z = 3$  Bethe lattice as in 1D systems.

Taking into account that the Bethe lattice is one of the standard models for the studying the limit of infinite dimensions, it would be very interesting to compare the present results for  $z = 3$  with the outcome of the  $d = \infty$  equations in order to quantify the importance of  $1/d$  corrections. Moreover, further DMRG investigations including NNN hoppings should be very valuable for a better understanding of the metal-insulator transition in the presence of frustrations, particularly since the information derived from the DMRG method is complementary to finite-temperature quantum Monte-Carlo calculations.

## ACKNOWLEDGMENTS

Computer resources provided by IDRIS (CNRS) under project No. 960806 are gratefully acknowledged.

## APPENDIX

The aim of this section is to outline the block diagonalization of the tight-binding matrix of a *finite* Bethe lattice formed by a central site  $i = 0$  and  $L$  successive nearest neighbor (NN) shells. The number of sites at shell  $l$  ( $1 \leq l \leq L$ ) is given by  $N_s(l) = z(z-1)^{l-1}$ , where  $z$  refers to the coordination number. The notation used for labelling the lattice sites is illustrated in Fig. 9 for  $z = 3$ .

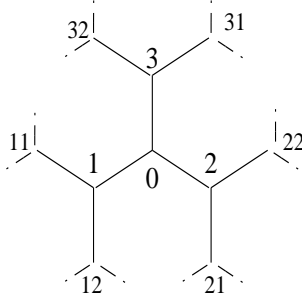


FIG. 9. Labelling of Bethe-lattice sites used in this appendix.

A site belonging to the shell  $l$  is denoted by the set of  $l$  numbers  $(i_1, i_2, \dots, i_l)$  which define the path to follow in order to reach the desired site starting from the central site  $i = 0$ . The tight-binding matrix  $H_0$  of the  $z = 3$  Bethe lattice with NN hoppings  $t$  can be block diagonalized by using that the finite Bethe lattice is invariant after the transposition of any pair of branches that connect a site of shell  $l-1$  with its 2 NN's of shell  $l$ . For the outermost shell ( $l = L$ ) the symmetry adapted single-particle states are

$$|i_1, i_2, \dots, i_{L-1}, +\rangle = (|i_1, i_2, \dots, i_{L-1}, 1\rangle + |i_1, i_2, \dots, i_{L-1}, 2\rangle) / \sqrt{2} \quad (4)$$

$$|i_1, i_2, \dots, i_{L-1}, -\rangle = (|i_1, i_2, \dots, i_{L-1}, 1\rangle - |i_1, i_2, \dots, i_{L-1}, 2\rangle) / \sqrt{2}. \quad (5)$$

For the other shells ( $l < L$ ) one proceeds recursively in the same way building symmetric and antisymmetric linear combinations. For the first shell the 3-fold symmetry around the central site  $i = 0$  is applied.

In the new basis  $H_0$  splits into a  $(L+1) \times (L+1)$  matrix block of the form

$$A = \begin{bmatrix} 0 & \sqrt{3}t & 0 & \dots & \\ \sqrt{3}t & 0 & \sqrt{2}t & 0 & \\ 0 & \sqrt{2}t & 0 & \sqrt{2}t & \\ \vdots & & \ddots & \ddots & \ddots \\ & & & \sqrt{2}t & 0 \end{bmatrix}, \quad (6)$$

which involves only purely even states including the central site, and in smaller  $l \times l$  matrices  $B_l$  with  $1 \leq l \leq L$  of the form

$$B_l = \begin{bmatrix} 0 & \sqrt{2}t & 0 & & \cdots \\ \sqrt{2}t & 0 & \sqrt{2}t & 0 & \\ 0 & \sqrt{2}t & 0 & \sqrt{2}t & \\ \vdots & & \ddots & \ddots & \ddots \\ & & & \sqrt{2}t & 0 \\ & & & \sqrt{2}t & 0 \end{bmatrix}. \quad (7)$$

$B_L$  appears twice in  $H_0$  and each of the other  $B_l$  appears  $3 \times 2^{L-l-1}$  instances in the total tight-binding matrix.

The eigenvalues of  $B_l$  are  $\beta_k = -2\sqrt{2}t \cos \frac{k\pi}{l+1}$  with  $k \in [1, l]$  and those of  $A$  are  $\alpha_k = -2\sqrt{2}|t| \cos \theta_k$  where the  $\theta_k$  are the roots of  $2 \sin(L+2)\theta = \sin L\theta$ . The later equation is solved numerically and the tight-binding energy per site  $E_s$  of the finite Bethe lattice is determined for any  $L$ . The extrapolated value for  $L \rightarrow \infty$  is  $E_s = -1.10306t$ . Notice that this result differs from the integral of the local density of states at the central site ( $E = -1.5255t$ ) since  $E_s(L \rightarrow \infty)$  is dominated by surface contributions.

<sup>1</sup> W. Metzner and D. Vollhardt, Phys. Rev. Lett. **62**, 324 (1989); D. Vollhardt, in *Correlated Electron Systems*, edited by V.J. Emery (World Scientific, Singapore, 1993).

<sup>2</sup> M.J. Rozenberg, X.Y. Zhang and G. Kotliar, Phys. Rev. Lett. **69**, 1236 (1992); M.J. Rozenberg, G. Kotliar and X.Y. Zhang, Phys. Rev. **B49**, 10181 (1994).

<sup>3</sup> A. Georges and W. Krauth, Phys. Rev. Lett. **69**, 1240 (1992); Phys. Rev. B **48**, 7167 (1993).

<sup>4</sup> J. Hong and H.Y. Kee, Phys. Rev. B **52**, 2415 (1995).

<sup>5</sup> S.R. White, Phys. Rev. Lett. **69**, 2863 (1992); Phys. Rev. B **48**, 10345 (1993).

<sup>6</sup> S.R. White and D.A. Huse, Phys. Rev. **B48**, 3844 (1993); K.A. Hallberg, P. Horsh, G. Martinez, Phys. Rev. **B52**, R719 (1995); S.R. White, Phys. Rev. **B53**, 52 (1996); S. Liang and H. Pang, Europhys. Lett. **32**, 173 (1995); S. Qin, S. Liang, Z. Su and L. Yu, Phys. Rev. B **52**, R5475 (1995); B. Srinivasan, S. Ramasesha and H.R. Krishnamurthy, Phys. Rev. B **54**, 2276 (1996); H. Pang and S. Liang, Phys. Rev. B **51**, 10287 (1995); M.-B. Lepetit and G.M. Pastor, Phys. Rev. B **56**, 4447 (1997); S.R. White, Phys. Rev. Lett. **69**, 2863 (1992); C.C. Yu, S.R. White, Phys. Rev. Lett. **71**, 3866 (1993); M. Guerrero, C.C. Yu, Phys. Rev. **B51**, 10301 (1995).

<sup>7</sup> H. Otsuka, Phys. Rev. B **53**, 14004 (1996).

<sup>8</sup> J. Hubbard, Proc. R. Soc. London **A276**, 238 (1963); **A281**, 401 (1964); J. Kanamori, Prog. Theo. Phys. **30**, 275 (1963); M.C. Gutzwiller, Phys. Rev. Lett. **10**, 159 (1963).

<sup>9</sup> E.H. Lieb, Phys. Rev. Lett. **62**, 1201 (1989).

<sup>10</sup> E.H. Lieb and F.Y. Wu, Phys. Rev. Lett. **20**, 1445 (1968).

<sup>11</sup> M.-B. Lepetit and G.M. Pastor, Phys. Rev. B **56**, 4447 (1997).